JOURNAL OF MEDICINAL FOOD
J Med Food 18 (1) 2015, 60–66

DOI: 10.1089/jmf.2014.0036

Investigating the Effects of Resveratrol on Chronically Ischemic Myocardium in a Swine Model of Metabolic Syndrome: A Proteomics Analysis

Ashraf A. Sabe, Ahmed A. Sadek, Nassrene Y. Elmadhun, Rahul S. Dalal, Michael P. Robich, Cesario Bianchi, and Frank W. Sellke

Division of Cardiothoracic Surgery, Cardiovascular Research Center, Warren Alpert School of Medicine, Brown University, Providence, Rhode Island, USA.

ABSTRACT Resveratrol has been shown to improve cardiac perfusion and ventricular function after chronic ischemic injury. Using proteomic analysis, we sought to objectively investigate potential mechanisms, by which resveratrol exerts its cardioprotective effects in the setting of metabolic syndrome and chronic myocardial ischemia. Yorkshire swine were divided into two groups based on diet: high cholesterol ($n=7$) or a high-cholesterol diet with supplemental resveratrol ($n=6$). Four weeks later, all animals underwent surgical placement of an ameroid constrictor to their left circumflex artery. Diets were continued for another 7 weeks, and then the ischemic myocardium was harvested for proteomics analysis. Proteomic analysis identified 669 common proteins between the two groups. Of these proteins, 76 were statistically different, of which 41 were characterized ($P<.05$). Pathway analysis demonstrated that in animals supplemented with resveratrol, there was a downregulation in several proteins involved with mitochondrial dysfunction, cell death, and unfavorable cardiac remodeling. Furthermore, there was an upregulation in proteins involved in free radical elimination. We conclude that resveratrol supplementation significantly alters several critical protein markers in the chronically ischemic myocardium. Further investigation of these proteins may help elucidate the mechanisms by which resveratrol exerts its cardioprotective effects.

KEY WORDS: • *ischemic heart disease* • *metabolic syndrome* • *metabolism* • *proteomics* • *remodeling* • *resveratrol*

INTRODUCTION

RESVERATROL IS BELIEVED TO be cardioprotective during chronic myocardial ischemia. This naturally occurring polyphenol is found in cocoa, peanuts, berries, and grapes used to make red wine.[1] The majority of studies investigating resveratrol have attributed its benefits to activation of mammalian sirtuins (SIRT1–7). Sirtuins are a highly conserved family of deacetylases involved in several essential cellular processes, including metabolic regulation and DNA repair.[2] The benefits of resveratrol are often attributed to its activation of SIRT1, which has been shown to mimic the benefits of caloric restriction. Acting on sirtuins, resveratrol has been shown to increase the lifespan and delay the expression of unfavorable aging-related phenotype in rodents.[3]

The mechanisms by which resveratrol exerts its cardioprotective effects remain under investigation. In animal models, reported benefits of resveratrol after ischemic injury include improvements in oxidative stress, infarct size, ventricular remodeling, and vascular dysfunction.[1,4] Although these findings have been well demonstrated in small animals, human studies are lacking. To help bridge this gap, we developed a clinically relevant swine model of metabolic syndrome and chronic myocardial ischemia.[4] With this model, we demonstrated that resveratrol supplementation decreased cardiac risk factors, including total cholesterol, inflammation, and insulin sensitivity in peripheral tissues.[5,6] Resveratrol was also shown to decrease ventricular wall motion dysfunction, improve myocardial perfusion, and increase microvascular relaxation.[7] To further characterize the effects of resveratrol, we performed a proteomics analysis on a chronically ischemic myocardium in a swine model with metabolic syndrome. We hypothesized that regulation of proteins in animals supplemented with resveratrol may provide mechanistic clues as to its cardioprotective effects.

MATERIALS AND METHODS

Animal model and surgical interventions

Adult male Yorkshire swine (Parsons Research, Amherst, MA, USA) were divided into two groups based on a daily diet fed over an 11-week period. The high-cholesterol control group (HCC, $n=7$) was given daily feedings of 500 g of a high-cholesterol diet providing 2248 kcal/day consisting of 75% regular chow, 4% cholesterol, 17.2% coconut

Manuscript received 5 March 2014. Revision accepted 18 June 2014.

Address correspondence to: Frank W. Sellke, MD, Division of Cardiothoracic Surgery, Cardiovascular Research Center, Warren Alpert School of Medicine, Brown University, 2 Dudley St., MOC 360 Providence, RI 02905, USA, E-mail: fsellke@lifespan.org

oil, 2.3% corn oil, and 1.5% sodium cholate. Animals in the experimental group were fed the same diet as the HCC animals but were also supplemented with daily oral resveratrol (HCRV; 100 mg/kg/day, $n=6$) (ChromaDex, Irvine, CA, USA). Feedings were observed to confirm complete consumption of chow and supplement. After 4 weeks, animals underwent surgical placement of a titanium ameroid constrictor (Research Instruments SW, Escondito, CA, USA) on the proximal left circumflex coronary artery (LCx). Seven weeks later, animals were euthanized and their hearts were harvested. Tissue samples from the chronically ischemic myocardium (LCx territory) were rapidly frozen in liquid nitrogen. All experiments were approved by the Institutional Animal Care and Use Committee of the Rhode Island Hospital. Animals were cared for in compliance with the Principles of Laboratory Animal Care formulated by the National Society for Medical Research and the Guide for the Care and Use of Laboratory Animals.

Myocardial perfusion and coronary angiography

The methods for myocardial perfusion analysis and coronary angiography have been previously described in these animals.[7] Briefly, just before ameroid placement, gold-labeled microspheres (Biophysics Assay Laboratory, Worcester, MA, USA) were injected into the left atrium, while the LCx was temporarily occluded. Lutetium and Europium isotope-labeled microspheres were injected at the final procedure at rest and when paced, respectively. At the conclusion of the study, microsphere densities were measured in tissue samples to localize the area at risk for ischemia and determine myocardial blood flow. Before euthanasia, the animals underwent coronary angiography to document occlusion of the left circumflex artery.[7]

Proteomics

Myocardial lysates. A sodium dodecyl sulfate (2%)-based detergent was used to isolate whole cell lysates from homogenized myocardial tissue in the chronically ischemic territories. The total protein concentration was determined by bicinchoninic acid assay (BCA assay; Pierce, Rockford, IL, USA).

Clean-up and in-solution digestion. Cell lysates were cleaned up to remove the detergent using the ReadyPrep 2-D Clean-Up Kit (Bio-Rad, Waltham, MA, USA). After clean-up, lyophilized protein pellets were reconstituted in 4 M urea/50 mM NH_4HCO_3 (Sigma-Aldrich, Natrick, MA, USA), reduced with 200 mM dithiothreitol (Thermo Scientific, San Jose, CA, USA)/0.1 M NH_4HCO_3 for 45 min at 37°C, alkylated with 0.5 M iodoacetamide (Sigma)/0.1 M NH_4HCO_3 for 30 min at room temperature in the dark, diluted with three volumes of 100 mM NH_4HCO_3, and then digested with trypsin (50 mM NH_4HCO_3/5 mM $CaCl_2$/0.1 mg/mL trypsin solution) overnight at 37°C. After digestion, peptides were acidified with 5% formic acid, dried in a vacuum centrifuge, and stored at −20°C until they were run on the liquid chromatography-mass spectometry (LC/MS).

Nano-LC-MS/MS analysis (Q Exactive OrbiTrap). Lysates prepared in tryptic peptides were fractionated with a C18 reversed-phase column (C18 PepMap 100, 75 μm ID × 15 cm, 3 μm particle size; Dionex/LC Packings, Vernon Hills, IL, USA) operating at a flow rate of 300 nL/min. Solvent A was 0.1% formic acid in water, and solvent B was 0.1% formic acid in acetonitrile. Peptides were eluted into the Q Exactive Orbitrap mass spectrometer (Thermo Scientific) directly using a reversed-phase gradient (0–35% solvent B over 40 min) through electrospray ionization. Full MS scans in the m/z range of 400–1800 at a nominal resolution of 70,000 were collected in the OrbiTrap, followed by data-dependent acquisition of MS/MS spectra for the 12 most abundant fragment ions. Employing a 15-sec dynamic exclusion time minimized repeated fragmentation of the same ion.

MS data analysis using Mascot and ProteoIQ and pathway analysis. MS/MS spectra were searched against the Uniprot pig protein database (downloaded May 2013) using the Mascot algorithm v.2.3.02 provided by Matrix Science, Inc. (Boston, MA, USA). The Uniprot pig database contained 52,280 protein entries (50% forward, 50% reversed). Mascot was performed with the following parameters: trypsin enzyme specificity, two possible missed cleavages, 10 ppm mass tolerance for precursor ions, and 20 mmu mass tolerance for fragment ions. Search parameters specified a differential modification of oxidation on methionine and a static modification of carbamidomethylation (+57.0215 Da) on cysteine. Protein quantification was performed using ProteoIQ software v. 2.3.05 (BioInquire, Bogart, GA, USA) with spectra count data. To provide high confidence on peptide sequence assignment and protein identification, data were filtered with the following stringent criteria: Mascot Ion score >20 for all charge states, 1% peptide false discovery rate (FDR), and 1% protein FDR. Bioinformatic and pathway

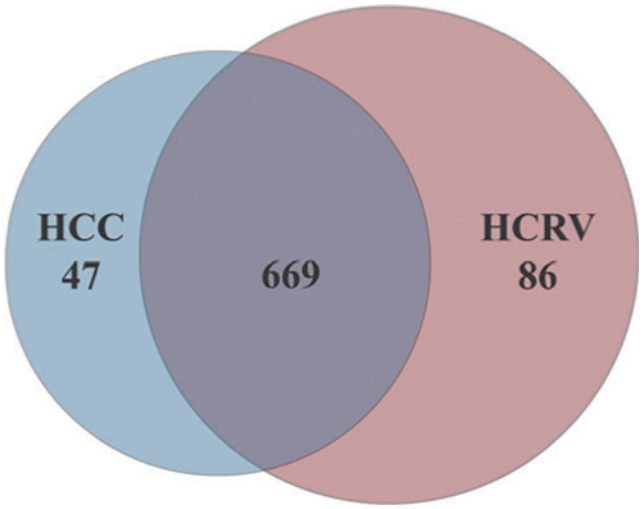

FIG. 1. Venn diagram demonstrating the number of proteins identified with proteomics in each group. Color images available online at www.liebertpub.com/jmf

analysis was performed with the aid of Ingenuity Pathway Analysis and Ingenuity iReport software (Ingenuity Systems, Inc., Redwood City, CA, USA) with a fold change cutoff of 1.

TUNEL assay

Frozen sections of myocardium were fixed in formalin and DNA breaks were identified according to the manufacturer's specifications using the ApoTag ISOL immunofluorescence kit (EMD Millipore, Billerica, MA, USA) for terminal deoxynucleotidyl transferase dUTP nick end labeling (TUNEL). Sections were mounted in Vectashield (Vector Laboratories, Inc., Burlingame, CA, USA) with 4′,6-diamidino-2-phenylindole (DAPI). Three 20× images from each section were taken and TUNEL-stained nuclei were counted. The results of the three images were averaged and expressed as nuclei per high-powered field.

Histologic examination

Staining quantification of Picosirius red staining on frozen tissue sections was measured using ImageJ software (National Institutes of Health, Bethesda, MD, USA). This process was repeated in duplicate for each animal. Representative

Table 1. Protein Expression in Ischemic Myocardium

Accession ID	*Protein name*	*HCC*	*HCRV*	P-*value*
Metabolic				
AK4	Adenylate kinase 4	1 ± 0.64	1.40 ± 0.00	.01
ATP5L	ATP synthase, H+ transporting, mitochondrial Fo complex, subunit G	1 ± 0.12	1.62 ± 0.25	.039
COX6C	Cytochrome c oxidase subunit VIc	1 ± 0.33	0.13 ± 0.14	.029
CRAT	Carnitine O-acetyltransferase	1 ± 0.10	0.70 ± 0.09	.054
DDT	D-dopachrome tautomerase	1 ± 0.65	3.50 ± 0.00	.0045
FABP3	Fatty acid binding protein 3, muscle, and heart (mammary-derived growth inhibitor)	1 ± 0.06	0.8 ± 0.053	.035
IDH3B	Isocitrate dehydrogenase 3 (NAD+) beta	1 ± 0.08	0.53 ± 0.10	.0032
MB	Myoglobin	1 ± 0.04	0.82 ± 0.07	.042
NDUFA4	NADH dehydrogenase (ubiquinone) 1 alpha subcomplex, 4, 9kDa	1 ± 0.10	0.56 ± 0.06	.0048
PGAM2	Phosphoglycerate mutase 2 (muscle)	1 ± 0.07	0.69 ± 0.08	.013
PKM	Pyruvate kinase, muscle	1 ± 0.11	1.2 ± 0.098	.022
POPDC2	Popeye domain containing 2	1 ± 0.47	1.94 ± 0.43	.04
PRDX2	Peroxiredoxin 2	1 ± 0.06	1.37 ± 0.08	.0026
PYGL	Phosphorylase, glycogen, liver	1 ± 0.12	1.42 ± 0.12	.036
SDHB	Succinate dehydrogenase complex, subunit B, iron sulfur (Ip)	1 ± 0.04	0.67 ± 0.08	.0037
SDHC	Succinate dehydrogenase complex, subunit C, integral membrane protein, 15kDa	1 ± 0.21	0.35 ± 0.16	.034
VAPB	VAMP (vesicle-associated membrane protein)-associated protein B and C	1 ± 0.18	0.39 ± 0.25	.01
Structural				
CAPZA2	Capping protein (actin filament) muscle Z-line, alpha 2	1 ± 0.11	0.68 ± 0.11	.0091
CHCHD3	Coiled-coil-helix-coiled-coil-helix domain containing 3	1 ± 0.07	0.43 ± 0.14	.0026
NEBL	Nebulette	1 ± 0.09	0.71 ± 0.05	.00027
PFN1	Profilin 1	1 ± 0.65	2.92 ± 0.64	.0091
TLN1	Talin 1	1 ± 0.30	2.53 ± 0.47	.017
TUBA1A	Tubulin, alpha 1a	1 ± 0.11	1.58 ± 0.23	.037
TUBA1B	Tubulin, alpha 1b	1 ± 0.07	1.39 ± 0.17	.047
TUBA4A	Tubulin, alpha 4a	1 ± 0.08	1.56 ± 0.23	.034
Miscellaneous				
BSG	Basigin (Ok blood group)	1 ± 0.18	0.39 ± 0.25	.01
CANX	Calnexin	1 ± 0.15	0.75 ± 0.14	.038
EEF1B2	Eukaryotic translation elongation factor 1 beta 2	1 ± 0.65	2.92 ± 0.64	.0091
GDI2	GDP dissociation inhibitor 2	1 ± 0.14	1.79 ± 0.27	.019
GNB2L1	Guanine nucleotide binding protein (G protein), beta polypeptide 2-like 1	1 ± 0.35	2.63 ± 0.39	.01
HNRNPH1	Heterogeneous nuclear ribonucleoprotein H1 (H)	1 ± 0.22	0.36 ± 0.11	.031
HSP90AA1	Heat shock protein 90 kDa alpha (cytosolic), class A member 1	1 ± 0.05	1.52 ± 0.24	.043
HSPA6	Heat shock 70 kDa protein 6 (HSP70B')	1 ± 0.06	0.71 ± 0.11	.03
PSME2	Proteasome (prosome, macropain) activator subunit 2 (PA28 beta)	1 ± 1.08	7.00 ± 1.81	.0031
PDIA4	Protein disulfide isomerase family A, member 4	1 ± 0.35	0.29 ± 0.32	.04
RPS12	Ribosomal protein S12	1 ± 0.35	0.29 ± 0.32	.04
RPS13	Ribosomal protein S13	1 ± 0.35	0.29 ± 0.29	.04
TMSB10	Thymosin beta 10	1 ± 0.20	0.72 ± 0.11	.011
TPM1	Tropomyosin 1 (alpha)	1 ± 0.04	0.82 ± 0.05	.016
TPM2	Tropomyosin 2 (beta)	1 ± 0.05	0.76 ± 0.08	.03
TPM3	Tropomyosin 3	1 ± 0.05	0.81 ± 0.07	.046

Protein expression listed as fold change ± SEM compared to HCC. *P*-value determined from a *t*-test.
HCC, high cholesterol control; HCRV, HCC supplemented with daily oral resveratrol.

images included on this article were obtained using Aperio ScanScope Technology (Aperio, Vista, CA, USA) and captured at 5 × magnification. The Pathology and Histology Core Facility at Rhode Island Hospital performed the tissue staining and the scanning.

Data analysis

Probability values (*P*-values) for the comparative proteomics data are reported from a *t*-test and were considered significant if less than .05. All results are expressed as fold change ± standard deviation or standard error of the mean, as compared to HCC.

RESULTS

Animal model

As previously reported, animals included for analysis survived to completion of the study. Before sacrifice, coronary catheterization was performed and demonstrated total occlusion of the left circumflex artery secondary to ameroid placement in all animals. Myocardial blood flow was decreased in the HCC group compared with the HCRV group after stress ventricular pacing.[7]

Proteomics data

A total of 802 proteins were identified in the ischemic myocardium with proteomic analysis. There were 47 unique proteins in the HCC group and 86 unique proteins in the HCRV group. There were 669 common proteins in both groups (Fig. 1). Out of these 669 proteins, 76 were found to be significantly different between the two groups, 41 of which are characterized (Table 1; $P < .05$).

Bioinformatics

A comparative analysis was performed on proteins found to have significant differences between the HCC and HCRV groups. Proteins identified have been divided into categories based on known cellular functions (Table 1 and Fig. 2; $P < .05$). Resveratrol supplementation resulted in a significant decrease in multiple proteins involved in mitochondrial dysfunction, including NADH dehydrogenase 1 alpha subcomplex 4, cytochrome c oxidase subunit VIc, and vesicle-associated membrane protein B (Table 2 and Fig. 2; $P = .0048$; $P = .029$; 0.01). The succinate dehydrogenase complexes, subunit B (SDHB) and subunit C (SDHC), involved in mitochondrial dysfunction and cell death, were also decreased with resveratrol supplementation (Table 2 and Fig. 2; $P = .0037$; $P = .034$). Other proteins known to be involved in cellular death were identified and found to be lower in animals treated with resveratrol. These proteins include thymosin beta 10, tropomyosin 1 (alpha), tropomyosin 3, myoglobin, and calnexin (Table 2 and Fig. 2; $P = .011$; $P = .016$; $P = .046$; $P = .042$; $P = .038$; respectively). Interestingly, proteins involved in cardiac remodeling were similarly decreased with resveratrol supplementation. These proteins include phosphoglycerate mutase 2, tropomyosin 1 (alpha), tropomyosin 2 (beta), nebulette, fatty acid binding protein 3, and myoglobin (Table 2 and Fig. 2; $P = .013$; $P = .016$; $P = .03$; $P = .00027$; $P = .035$; $P = .042$; respectively). Resveratrol supplementation also resulted in an increase in peroxiredoxin 2, a protein involved in free radical scavenging (Table 2 and Fig. 2; $P = .0026$).

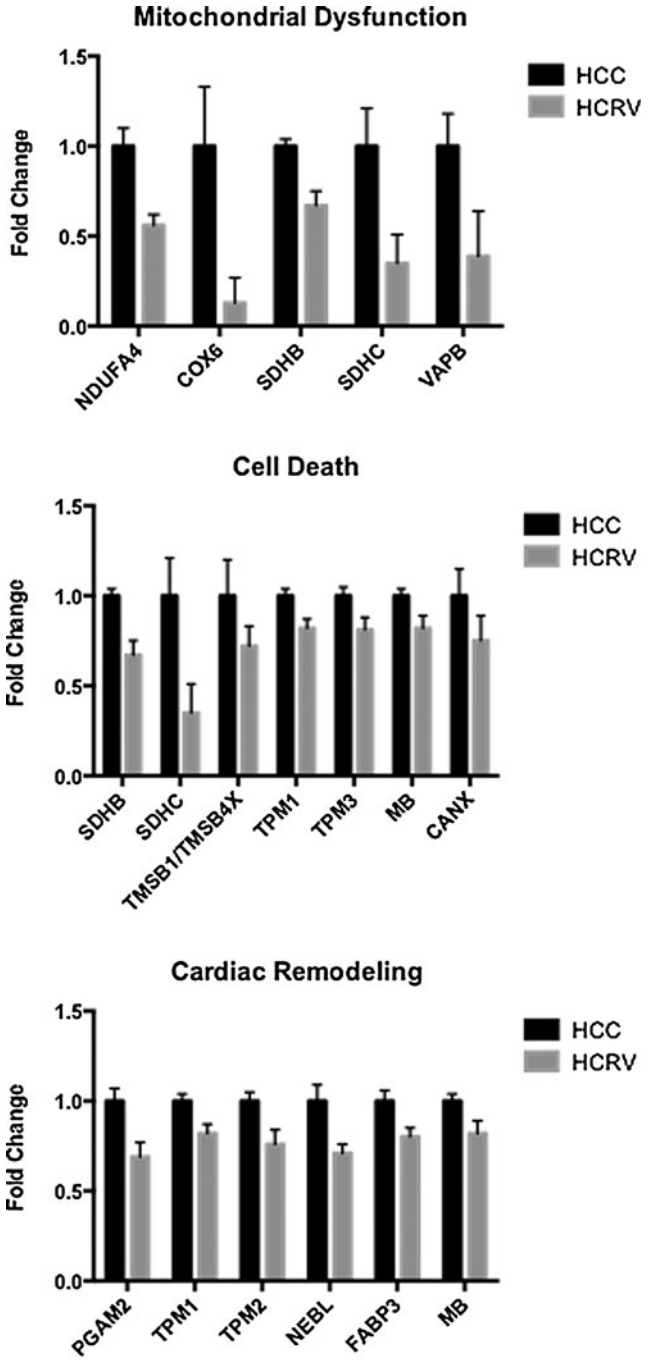

FIG. 2. Protein expression grouped by potential pathophysiologic function. Compared with the HCC group, in the HCRV group, there was a significant decrease in several protein markers associated with mitochondrial dysfunction, cell death, and cardiac remodeling. Protein expression listed as fold change ± SEM compared to HCC. *P*-value determined from a *t*-test. All values represented are significant ($P < .05$). HCC, high cholesterol control; HCRV, HCC supplemented with daily oral resveratrol.

Table 2. Protein Expression in Ischemic Myocardium Grouped by Potential Pathophysiologic Function

Accession ID	*Protein name*	*HCC*	*HCRV*	P-*value*
Mitochondrial dysfunction				
NDUFA4	NADH dehydrogenase (ubiquinone) 1 alpha subcomplex, 4, 9kDa	1 ± 0.10	0.56 ± 0.06	.0048
COX6C	Cytochrome c oxidase subunit VIc	1 ± 0.33	0.13 ± 0.14	.029
SDHB	Succinate dehydrogenase complex, subunit B, iron sulfur (Ip)	1 ± 0.04	0.67 ± 0.08	.0037
SDHC	Succinate dehydrogenase complex, subunit C, integral membrane protein, 15kDa	1 ± 0.21	0.35 ± 0.16	.034
VAPB	VAMP (vesicle-associated membrane protein)-associated protein B and C	1 ± 0.18	0.39 ± 0.25	.01
Cell death				
SDHB	Succinate dehydrogenase complex, subunit B, iron sulfur (Ip)	1 ± 0.04	0.67 ± 0.08	.0037
SDHC	Succinate dehydrogenase complex, subunit C, integral membrane protein, 15kDa	1 ± 0.21	0.35 ± 0.16	.034
TMSB1/TMSB4X	Thymosin beta 10	1 ± 0.20	0.72 ± 0.11	.011
TPM1	Tropomyosin 1 (alpha)	1 ± 0.04	0.82 ± 0.05	.016
TPM3	Tropomyosin 3	1 ± 0.05	0.81 ± 0.07	.046
MB	Myoglobin	1 ± 0.04	0.82 ± 0.07	.042
CANX	Calnexin	1 ± 0.15	0.75 ± 0.14	.038
Cardiac remodeling				
PGAM2	Phosphoglycerate mutase 2 (muscle)	1 ± 0.07	0.69 ± 0.08	.013
TPM1	Tropomyosin 1 (alpha)	1 ± 0.04	0.82 ± 0.05	.016
TPM2	Tropomyosin 2 (beta)	1 ± 0.05	0.76 ± 0.08	.03
NEBL	Nebulette	1 ± 0.09	0.71 ± 0.05	.00027
FABP3	Fatty acid binding protein 3, muscle, and heart (mammary-derived growth inhibitor)	1 ± 0.06	0.80 ± 0.05	.035
MB	Myoglobin	1 ± 0.04	0.82 ± 0.07	.042
Free radical scavenging				
PRDX2	Peroxiredoxin 2	1 ± 0.06	1.37 ± 0.08	.0026

Protein expression listed as fold change ± SEM compared to HCC. *P*-value determined from a *t*-test.

Apoptosis and myocardial fibrosis

Apoptosis in the ischemic myocardium, assessed by TUNEL staining, was slightly decreased in the HCRV group compared with the HCC group, although the change was not statistically significant ($P = .55$; Fig. 3). However, as demonstrated by Picosirius red staining, intramyocardial fibrosis was significantly decreased in the HCRV group compared with the HCC group ($P < .001$; Fig. 4).

DISCUSSION

In a swine model with metabolic syndrome and chronic myocardial ischemia, we demonstrate that resveratrol supplementation significantly alters the levels of several key proteins involved in metabolism, cell death, and structural remodeling and decreases myocardial fibrosis. These findings are consistent with our previous work demonstrating that resveratrol modifies risk factors for cardiac disease,

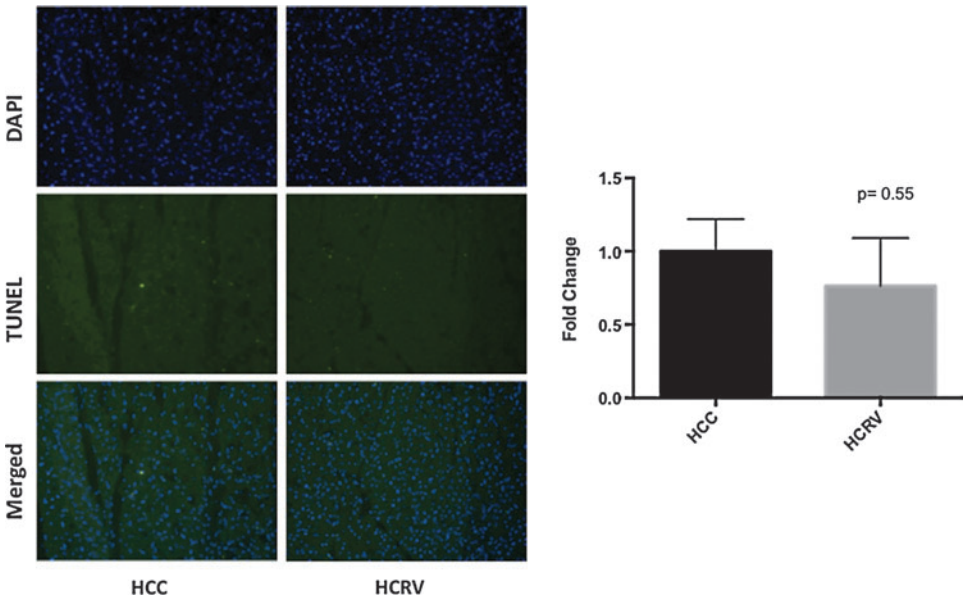

FIG. 3. Terminal deoxynucleotidyl transferase dUTP nick end labeling (TUNEL) staining in a chronically ischemic myocardium. Color images available online at www.liebertpub.com/jmf

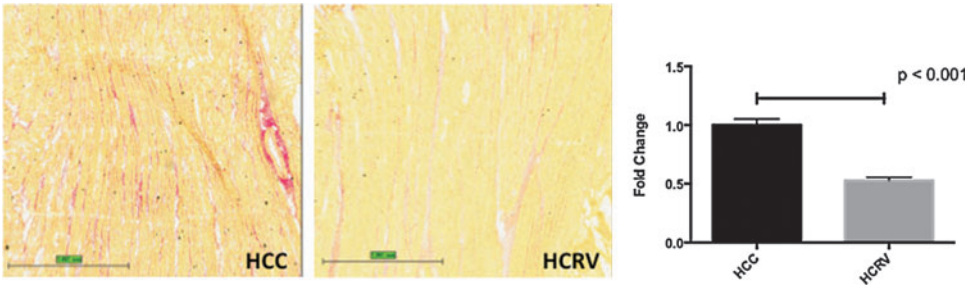

FIG. 4. Picosirius red staining for fibrosis in a chronically ischemic myocardium. Color images available online at www.liebertpub.com/jmf

improves global ventricular functioning, and increases microvascular relaxation.[6,7]

Our group and others have attempted to better define the mechanism by which resveratrol exerts these benefits.[7–10] These effects are thought to occur through multiple pathways, including induction of nitric oxide synthase and reduction of superoxide production by inhibiting the NADH/NADPH oxidase activity in mitochondria.[1,8] This pathway may also be a mechanism by which resveratrol induces its antioxidant effects.

We also demonstrated that resveratrol supplementation significantly attenuates several protein markers known to induce mitochondrial dysfunction (Table 2 and Fig. 2). Notable proteins identified include the succinate dehydrogenase complexes (SDHB and SDHC). These proteins are associated with the electron transport chain in mitochondria, and mutations of the gene coding for these proteins can result in overproduction of superoxide radicals and result in oxidative stress, which leads to apoptosis.[11,12] Interestingly, we found a decrease in these proteins in animals supplemented with resveratrol. Similarly, animals supplemented with resveratrol also had a decrease in calnexin. Calnexin deficiency has been shown to be protective against endoplasmic reticulum stress-induced apoptosis.[13] Moreover, animals given resveratrol had an increase in peroxiredoxin 2. This protein is a known scavenger of free radicals, improves lipid metabolism, and has been shown to decrease apoptosis.[14,15]

In rodent models, resveratrol has been shown to prevent and reverse cardiac remodeling.[16,17] It has been demonstrated that tropomyosin mutations are associated with abnormal calcium binding and ventricular remodeling.[18] We noted a significant decrease in tropomyosin 1 (alpha) and tropomyosin 2 (beta) in animals given resveratrol. Similarly, nebulette was decreased in animals supplemented with resveratrol. Nebulette mutations have also been associated with dilated cardiomyopathy and heart failure.[19] After ischemic insult, especially in the setting of metabolic syndrome, overexpression of these proteins may result in increased maladaptive cardiac remodeling and resveratrol supplementation and, by decreasing these integral proteins, may ameliorate remodeling. It is important to note that there may be a significant overlap in these processes. For instance, overexpression of proteins that result in disturbances in mitochondrial homeostasis can lead to increased reactive oxygen species, triggering cell death pathways and unfavorable remodeling.

Limitations

There are limitations to this study. As this is a large animal model, the number of animals in each group was kept to a minimum while retaining appropriate statistical power. Although proteomics allows for a more objective identification of hundreds of proteins, the relevance of these proteins remains difficult to ascertain. As described in the methods, we did utilize strict identification criteria and an adequate number of subjects to limit the signal versus noise error; however, this remains a limitation in any mass spectrometry study. To help determine the most relevant changes, we sorted proteins based on statistical significance before the bioinformatics analysis. It is important to note that posttranslational modifications of proteins that were not investigated in this project may also play important roles in cardioprotection, even though their protein levels were not significantly altered. In addition, the functions of many of the proteins identified in this project remain poorly understood, and their functions may be species and tissue dependent. The cause–effect relationship of these proteins within their respective networks, and in the setting of metabolic syndrome, needs further investigation.

In summary, through the use of proteomic analysis, we demonstrated a number of significant alterations in protein expression in the chronically ischemic myocardium of swine with metabolic syndrome. It is important to note that many of these proteins and networks remain poorly understood. These findings may guide further studies investigating the cardioprotective effects of resveratrol.

ACKNOWLEDGMENTS

Funding for this research was provided by the National Heart, Lung, and Blood Institute (R01HL46716, R01HL69024, and R01HL85647, Dr. F.W.S.), NIH Training grant 5T32-HL094300-03 (Dr. A.A.S. and Dr. N.Y.E.), and NIH Training grant T32-HL0074 (Dr. M.P.R.).

AUTHOR DISCLOSURE STATEMENT

No competing financial interests exist.

REFERENCES

1. Chu LM, Lassaletta AD, Robich MP, Sellke FW: Resveratrol in the prevention and treatment of coronary artery disease. *Curr Atheroscler Rep* 2011;13:439–446.

2. Price NL, Gomes AP, Ling AJ, *et al.*: SIRT1 is required for AMPK activation and the beneficial effects of resveratrol on mitochondrial function. *Cell Metab* 2012;15:675–690.
3. Baur JA, Pearson KJ, Price NL, *et al.*: Resveratrol improves health and survival of mice on a high-calorie diet. *Nature* 2006;444:337–342.
4. Elmadhun NY, Sabe AA, Robich MP, Chu LM, Lassaletta AD, Sellke FW: The pig as a valuable model for testing the effect of resveratrol to prevent cardiovascular disease. *Ann NY Acad Sci* 2013;1290:130–135.
5. Burgess TA, Robich MP, Chu LM, Bianchi C, Sellke FW: Improving glucose metabolism with resveratrol in a swine model of metabolic syndrome through alteration of signaling pathways in the liver and skeletal muscle. *Arch Surg* 2011;146:556–564.
6. Robich MP, Osipov RM, Chu LM, *et al.*: Resveratrol modifies risk factors for coronary artery disease in swine with metabolic syndrome and myocardial ischemia. *Eur J Pharmacol* 2011;664: 45–53.
7. Robich MP, Osipov RM, Nezafat R, *et al.*: Resveratrol improves myocardial perfusion in a swine model of hypercholesterolemia and chronic myocardial ischemia. *Circulation* 2010;122:S142–S149.
8. Baur JA, Sinclair DA: Therapeutic potential of resveratrol: the *in vivo* evidence. *Nat Rev Drug Discov* 2006;5:493–506.
9. Sabe AA, Elmadhun NY, Robich MP, Dalal RS, Sellke FW: Does resveratrol improve insulin signaling in chronically ischemic myocardium? *J Surg Res* 2013;183:531–536.
10. Sabe AA, Elmadhun NY, Dalal RS, Robich MP, Sellke FW: Resveratrol regulates autophagy signaling in chronically ischemic myocardium. *J Thorac Cardiovasc Surg* 2014;147:792–798; Discussion 798–799.
11. Slane BG, Aykin-Burns N, Smith BJ, *et al.*: Mutation of succinate dehydrogenase subunit C results in increased $O_2^{\bullet -}$, oxidative stress, and genomic instability. *Cancer Res* 2006;66:7615–7620.
12. Ishii N, Ishii T, Hartman PS: The role of the electron transport gene SDHC on lifespan and cancer. *Exp Gerontol* 2006;41:952–956.
13. Zuppini A, Groenendyk J, Cormack LA, *et al.*: Calnexin deficiency and endoplasmic reticulum stress-induced apoptosis. *Biochemistry* 2002;41:2850–2858.
14. Cha MK, Yun CH, Kim IH: Interaction of human thiol-specific antioxidant protein 1 with erythrocyte plasma membrane. *Biochemistry* 2000;39:6944–6950.
15. Yang S, Luo A, Hao X, *et al.*: Peroxiredoxin 2 inhibits granulosa cell apoptosis during follicle atresia through the NFKB pathway in mice. *Biol Reprod* 2011;84:1182–1189.
16. Xuan W, Wu B, Chen C, *et al.*: Resveratrol improves myocardial ischemia and ischemic heart failure in mice by antagonizing the detrimental effects of fractalkine. *Crit Care Med* 2012;40:3026–3033.
17. Kanamori H, Takemura G, Goto K, *et al.*: Resveratrol reverses remodeling in hearts with large, old myocardial infarctions through enhanced autophagy-activating AMP kinase pathway. *Am J Pathol* 2013;182:701–713.
18. Karibe A, Tobacman LS, Strand J, *et al.*: Hypertrophic cardiomyopathy caused by a novel alpha-tropomyosin mutation (V95A) is associated with mild cardiac phenotype, abnormal calcium binding to troponin, abnormal myosin cycling, and poor prognosis. *Circulation* 2001;103:65–71.
19. Chopra N, Knollmann BC: Genetics of sudden cardiac death syndromes. *Curr Opin Cardiol* 2011;26:196–203.